Single-Anchor Localizability in 5G Millimeter Wave Networks

Christopher E. O'Lone, Harpreet S. Dhillon, and R. Michael Buehrer

***Abstract*—Fifth generation networks utilizing millimeter wave frequencies enable single-anchor localization to be performed via a line-of-sight (LOS) path or, as recently suggested, via non-line-of-sight (NLOS) paths exclusively. Thus, for a single base station-mobile pair, under a Boolean model (random positions, sizes, and orientations) of reflectors, and considering first-order reflections (in addition to the LOS path), this paper analytically derives the probability that the mobile is able to obtain an unambiguous location estimate (*i.e.*, the mobile's *localizability*). This analysis also reveals that localization, via NLOS signals exclusively, is a relatively small contributor to the mobile's overall localizability.**

***Index Terms*—Localization, non-line-of-sight (NLOS), stochastic geometry, Boolean model, Poisson point process (PPP), millimeter wave (mm-wave), first-order reflection, 5G.**

I. Introduction

Emerging fifth generation (5G), millimeter wave (mm-wave) wireless networks with massive multiple-input multiple-output (MIMO) have fueled a resurgence in localization research. Specifically, the ability to obtain Angle-of-Departure (AOD) and Angle-of-Arrival (AOA) information through the use of beamforming and antenna arrays opens the possibility of performing single-anchor localization. Recent work in [1] reveals that even in the absence of an LOS path, an unambiguous location estimate can still be obtained from a single anchor if two or more NLOS paths are present (three or more if the relative orientations of the Tx and Rx need to be estimated, *i.e.*, situations where the devices do not know 'true north'). Since diffraction effects are negligible at mm-wave frequencies [2], reflections are the key enabler allowing for these NLOS paths to be harnessed for localization.

In order to incorporate reflections into an analysis of the mobile's localizability, we utilize an important tool from stochastic geometry; the Boolean model, which characterizes the random placements, sizes, and orientations of buildings in a network. This model has recently gained popularity in the study of propagation, channel characteristics, and performance metrics in mm-wave networks. Its use in this regard was pioneered in [3], and shortly thereafter, various versions of this model have been used to study the effects of first-order reflections on the power delay profile [4], [5], the total received interference power [6], and coverage probability [7].

While the Boolean model with first-order reflections has been used to investigate communications metrics, its use in studying localization metrics is limited to [8], where the model was used to study NLOS bias error in range measurements. Thus, this paper aims to leverage this model in the study of another localization performance metric: a device's *localizability* [9], *i.e.*, the probability that, for a given localization strategy, the device receives at least the minimum number of localization signals needed to obtain an unambiguous location estimate.[1,2] While localizability has been studied in 4G networks [9], this fundamental metric has yet to be examined in the context of 5G, mm-wave networks.

Contributions: For a single anchor-mobile pair, the mobile's localization probability is analytically derived; assuming mm-waves subject to blockages and reflections under the Boolean model and taking into account the possibility for localization via a single LOS signal or via several NLOS signals [1]. In obtaining this probability, we intermediately arrive at a similar metric from [6]: the average number of reflectors producing hearable, visible (*i.e.*, unblocked) reflections between the base station and mobile. However, given our interest in localization, an alternate derivation is presented, which is direct and potentially more illustrative for analyzing localization metrics that often require knowledge of multiple arriving paths at the receiver. Lastly, a numerical analysis demonstrates the efficacy and accuracy of this localizability result, and also reveals the minor contribution that NLOS localization plays in the overall localization probability, a result hinted at in [7] while studying coverage under an alternate setup.

Notation: All constructions and derivations are in $\mathbb{R}^2$ unless stated otherwise. Notation is as follows: lowercase, bold letters, *e.g.*, $\mathbf{x}$, represent vectors; $[\mathbf{x}]_i$ denotes the i^{th} component; $\mathbf{x}^T$ the transpose; $\mathbf{0}$ the zero vector; $\|\cdot\|$ the Euclidean norm; $\mathbf{R}(\theta) = \left[\begin{smallmatrix} \cos\theta & \sin\theta \\ -\sin\theta & \cos\theta \end{smallmatrix}\right]$ the rotation matrix which rotates the coordinate axes counterclockwise by angle θ; $\mathcal{L}_{[\mathbf{p},\mathbf{q}]}$ indicates the set of points forming a line segment between $\mathbf{p}$ and $\mathbf{q}$ (inclusive); similarly, the same notation with a letter other than $\mathcal{L}$, *e.g.*, $C_{[\mathbf{p},\mathbf{q}]}$, indicates the set of points along the curve, C, between the points $\mathbf{p}$ and $\mathbf{q}$; if $\mathcal{A} \subset \mathbb{R}^n$, then $\partial\mathcal{A}$ represents $\mathcal{A}$'s boundary (closure minus interior) and $\mu_n(\mathcal{A})$ the n-dimensional Lebesgue measure; if Φ is a Poisson point process (PPP), then $\Phi(\mathcal{A})$ denotes the number of points of Φ in $\mathcal{A}$; '$\mathbf{g}(x)$' denotes a vector function of a scalar, '$g(\mathbf{x})$' a scalar function of a vector, etc.

II. System Model

This section constructs the stochastic model for reflectors (buildings), describes the setup, and lists the assumptions used throughout the remainder of the paper.

Definition 1. *(Minkowski Sum [3])* For compact sets $\mathcal{A}, \mathcal{B} \subset \mathbb{R}^2$, the *Minkowski sum* is defined as

$$\mathcal{A} \oplus \mathcal{B} \triangleq \left\{ \mathbf{x} + \mathbf{y} \in \mathbb{R}^2 \;\middle|\; \mathbf{x} \in \mathcal{A},\; \mathbf{y} \in \mathcal{B} \right\}.$$

Definition 2. *(Reflector $R_{w,\theta,\mathbf{c}}$)* A square *reflector* with finite width, $w > 0$, orientation, $\theta \in (0, \pi/2)$, and center point, $\mathbf{c}$, is given by

$$R_{w,\theta,\mathbf{c}} \triangleq \bigcap_{i=\mathrm{I}}^{\mathrm{IV}} \left\{ \mathbf{x} \in \mathbb{R}^2 \;\middle|\; \mathbf{k}_i^T (\mathbf{x} - [\mathbf{c} - \mathbf{k}_i]) \geq 0 \right\},$$

where the $\mathbf{k}_i$ are given in Fig. 1(a).

Definition 3. (*Boolean Model, Generated by $R_{W,\Theta,\mathbf{0}}$*) Let $\Phi = \{\mathbf{c}_i\}_{i=1}^{\infty}$ be a *homogeneous* PPP over $\mathbb{R}^2$ with intensity λ and

The authors are with Wireless@VT, ECE Department, Virginia Tech, Blacksburg, VA 24061 USA (Email: {olone, hdhillon, buehrer}@vt.edu).

The work of H. S. Dhillon was supported by U.S. NSF Grant ECCS-1731711.

[1]The minimum number is, of course, determined via the noiseless case.

[2]We use 'localizability' and 'localization probability' interchangeably.

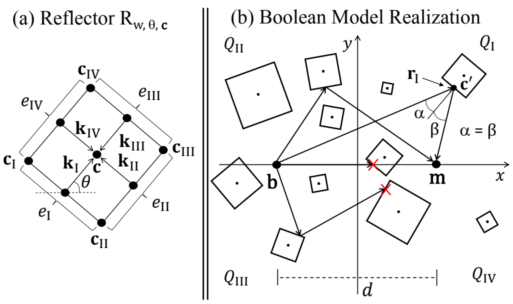

Fig. 1. SYSTEM MODEL. (a): The corners $\mathbf{c}_I$, $\mathbf{c}_{II}$, $\mathbf{c}_{III}$, & $\mathbf{c}_{IV}$ help define the edge sets: $e_I = \mathcal{L}_{[\mathbf{c}_I,\mathbf{c}_{II}]}$, $e_{II} = \mathcal{L}_{[\mathbf{c}_{II},\mathbf{c}_{III}]}$, etc. The vectors $\mathbf{k}_i$ (implicitly functions of w & θ) represent the displacement between the center of the reflector and the center of the corresponding edge. For reference, $\mathbf{k}_I$ always has angle θ and emanates from the center of e_I. The remaining $\mathbf{k}_i$ and e_i are labeled in increasing order counterclockwise. The edges dictate the Roman numeral labels – they are labeled according to the quadrant they produce reflections in, *e.g.*, in (b), e_I facilitates reflections in the 1st quadrant, Q_I. (b): Without loss of generality, the base station is placed at $\mathbf{b} = [-d/2, 0]^T$ and the mobile at $\mathbf{m} = [d/2, 0]^T$. We have: $Q_I = \{[x, y]^T \in \mathbb{R}^2 \mid x \geq 0, y \geq 0\}$, and the remaining quadrants are defined analogously, *i.e.* points on the axes are in more than one quadrant. Depicted are two NLOS paths, one blocked NLOS path, and a blocked LOS path. For reflections, the incident angle, α, equals the reflection angle, β. The reflection point in Q_I is denoted $\mathbf{r}_I \in \partial R_{w,\theta,\mathbf{c}'}$.

let the bivariate, discrete distribution $f_{W,\Theta}(w, \theta)$, with support $\text{supp}(f_{W,\Theta}) = \left\{ [w, \theta]^T \in \mathbb{R}^2 \;\middle|\; w \in \{w_i\}_{i=1}^{n_w},\; \theta \in \{\theta_j\}_{j=1}^{n_\theta} \right\}$, be the distribution from which a reflector's width and orientation are sampled.[3] Then, the *Boolean model, generated by $R_{W,\Theta,\mathbf{0}}$*, is defined by

$$\mathcal{B} \triangleq \bigcup_{i=1}^{\infty} \Big(\{\mathbf{c}_i\} \oplus R_{W_i,\Theta_i,\mathbf{0}} \Big), \text{ where } \mathbf{c}_i \in \Phi,\; \begin{bmatrix} W_i \\ \Theta_i \end{bmatrix} \overset{\text{i.i.d.}}{\sim} f_{W,\Theta},$$

and the reflectors are independent of Φ. (See Fig. 1(b).)

Next, we make the following assumptions:

1) Only first-order reflections whose total traversed path length is $\leq d_{max}$ meters are assumed to be detectable at the mobile. Effects of higher-order (*i.e.* multiple-bounce) reflections are ignored, a consequence of added reflection losses and increased pathloss [4].[4] Note, $d < d_{max}$.
2) Localization is performed during the initial access phase [1]. Thus, the base station is assumed to have 360° coverage, *i.e.*, a scan of the environment illuminates all possible reflection paths and allows for AOD estimation. The mobile is assumed to be equipped with an antenna array which can resolve the incoming signals' AOA [1].
3) Blocking is treated independently on all paths.[5] For reflected paths, blockages on the incident path are assumed to be independent of those on the reflected path.[6]
4) When LOS is blocked, it is assumed that at least two NLOS reflections are needed for localization [1].

III. Geometric Implications of the System Model

The Boolean model and assumptions in the previous section lead to important geometric consequences regarding where reflectors may be placed such that a first-order reflection is established. For a reflector $R_{w,\theta,\mathbf{c}}$, with w and θ *fixed* and $\mathbf{c}$ *arbitrary*, and ignoring blockages, this section characterizes the region where $\mathbf{c}$ can fall such that $R_{w,\theta,\mathbf{c}}$ can facilitate a reflection between $\mathbf{b}$ and $\mathbf{m}$. This 'reflection region,' constructed in [8], is briefly summarized in Definition 5.

To find this region, we first ask: Where are all of the points in $\mathbb{R}^2$ such that $\partial R_{w,\theta,\mathbf{c}}$ can intersect to facilitate a reflection, such as that in Q_I of Fig. 1(b)? Well, it turns out that all of these possible reflection points for $R_{w,\theta,\mathbf{c}}$ lie on a hyperbola:

Lemma 1. *(The Reflection Hyperbola [8]) Let $\theta \in (0, \pi/2)$, $\mathbf{b}$ and $\mathbf{m}$ be given as in Fig. 1(b), and let $\mathcal{H}_\theta$ be the set of all possible reflection points for $R_{w,\theta,\mathbf{c}}$. Then,*

$$\mathcal{H}_\theta = \Big\{ [x, y]^T \in \mathbb{R}^2 \;\Big|\; y^2 - x^2 + 2\cot(2\theta) xy + d^2/4 = 0 \Big\}.$$

Proof. Please refer to [8]. ■

Remark. Consequently, for $R_{w,\theta,\mathbf{c}}$ to facilitate a first-order reflection, it is both necessary and sufficient that $\exists i \in \{\text{I, II, III, IV}\}$ such that for $e_i \subset \partial R_{w,\theta,\mathbf{c}}$, $(e_i \cap Q_i \cap \mathcal{H}_\theta) \neq \emptyset$. See Fig. 2 for an example of $\mathcal{H}_\theta$.

Next, by Assumption 1, we only consider reflection points which correspond to reflections of distance $\leq d_{max}$. This implies that all reflection points of interest must lie within an ellipse with foci $\mathbf{b}$ and $\mathbf{m}$, called the 'hearable region.'

Definition 4. (*Hearable Region*) The *hearable region* is defined as $\mathcal{E}_{d_{max}} \triangleq \left\{ [x, y]^T \in \mathbb{R}^2 \;\middle|\; x^2/u^2 + y^2/v^2 \leq 1 \right\}$, where $u^2 = d_{max}^2/4$ and $v^2 = (d_{max}^2 - d^2)/4$.

It is now straightforward to find the region where $\mathbf{c}$ must lie in order for $R_{w,\theta,\mathbf{c}}$ to establish a reflection (of distance $\leq d_{max}$) between $\mathbf{b}$ and $\mathbf{m}$. This is called the *reflection region*:

Definition 5. *(Reflection Region for $R_{w,\theta,\mathbf{c}}$ [8])* Consider the four quadrant portions of the reflection hyperbola within $\mathcal{E}_{d_{max}}$: $\mathcal{H}_{\theta[\mathbf{m},\mathbf{h}_I]}$ for Q_I, $\mathcal{H}_{\theta[\mathbf{b},\mathbf{h}_{II}]}$ for Q_{II}, $\mathcal{H}_{\theta[\mathbf{b},\mathbf{h}_{III}]}$ for Q_{III}, and $\mathcal{H}_{\theta[\mathbf{m},\mathbf{h}_{IV}]}$ for Q_{IV}, where $\mathbf{h}_i \in \mathcal{H}_\theta \cap \partial\mathcal{E}_{d_{max}}$, $\forall i \in \{\text{I, II, III, IV}\}$. These $\mathbf{h}_i$ are given by

$$\mathbf{h}_I = \left[\sqrt{z_{I,III}}, \frac{v}{u}\sqrt{u^2 - z_{I,III}} \right]^T, \; \mathbf{h}_{II} = \left[-\sqrt{z_{II,IV}}, \frac{v}{u}\sqrt{u^2 - z_{II,IV}} \right]^T,$$

$\mathbf{h}_{III} = -\mathbf{h}_I$, and $\mathbf{h}_{IV} = -\mathbf{h}_{II}$, where

$$z_{I,III} = \frac{d_{max}^4 \cot^2\theta}{4\left[d_{max}^2 \csc^2\theta - d^2\right]}, \quad z_{II,IV} = \frac{d_{max}^4 \tan^2\theta}{4\left[d_{max}^2 \sec^2\theta - d^2\right]},$$

and u and v are from Definition 4. Next, consider dismantling the four edges comprising $\partial R_{w,\theta,\mathbf{c}}$ and placing their centers at the origin, preserving their respective orientations. We denote these translated edge-sets as: $e_{i,\mathbf{0}} = e_i + (\mathbf{k}_i - \mathbf{c})$. Since any point along an edge of $R_{w,\theta,\mathbf{c}}$ can induce a reflection by intersecting $\mathcal{H}_\theta$ in the proper quadrant, we define the *reflection region* as

$$\Omega(w, \theta, d_{max}) \triangleq \bigcup_{i=\text{I}}^{\text{IV}} \Big(\Omega_i + \mathbf{k}_i \Big), \quad \text{where}$$

$$\Omega_I \triangleq \mathcal{H}_{\theta[\mathbf{m},\mathbf{h}_I]} \oplus e_{I,\mathbf{0}}, \qquad \Omega_{II} \triangleq \mathcal{H}_{\theta[\mathbf{b},\mathbf{h}_{II}]} \oplus e_{II,\mathbf{0}}$$
$$\Omega_{III} \triangleq \mathcal{H}_{\theta[\mathbf{b},\mathbf{h}_{III}]} \oplus e_{III,\mathbf{0}}, \quad \Omega_{IV} \triangleq \mathcal{H}_{\theta[\mathbf{m},\mathbf{h}_{IV}]} \oplus e_{IV,\mathbf{0}}.$$

Remark. The notation $\Omega(w, \theta, d_{max})$ emphasizes that this region is dependent on these parameters. We may similarly write $\Omega_i(w, \theta, d_{max})$ for the four quadrant portions. Note $\mu_2\Big((\Omega_i(w, \theta, d_{max}) + \mathbf{k}_i) \cap (\Omega_j(w, \theta, d_{max}) + \mathbf{k}_j) \Big) = 0$, for $i, j \in \{\text{I, II, III, IV}\}$ and $i \neq j$. See Fig. 2 for a partial depiction.

[3] The integers n_w and n_θ are positive and finite.

[4] In practice, it is possible that a detectable higher-order reflection reaches the mobile, however, this scenario is rare and is not considered in this analysis.

[5] Independent blocking is a common assumption in the literature [4], [5], [6], as *dependent* blocking, where a single reflector may be responsible for blocking two or more paths, is difficult to model analytically.

[6] This is in contrast to [4], [5], and [6], where blocking is independent, but the entire reflected path is treated contiguously.

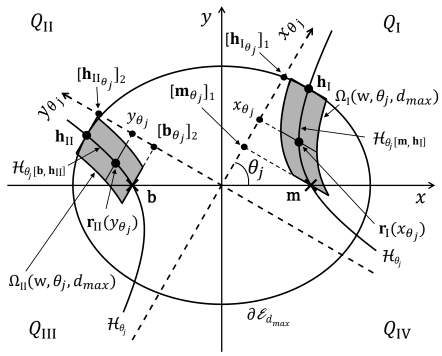

Fig. 2. Reflection Region in 1st & 2nd Quadrants (Shifted). For $R_{w,\theta_j,\mathbf{c}}$, the grayed region, $\Omega_{\mathrm{I}}(w, \theta_j, d_{max})$, depicts all of the points that *the center of its edge,* e_{I}, must lie in order to facilitate a reflection (of length $\leq d_{max}$) between $\mathbf{b}$ & $\mathbf{m}$. Likewise for $\Omega_{\mathrm{II}}(w, \theta_j, d_{max})$ and $R_{w,\theta_j,\mathbf{c}}$'s edge e_{II}. The subscript θ_j denotes coordinates in the rotated system. Here, $\theta_j = \pi/3$.

IV. The Localization Probability

We begin by covering some implications of Assumption 3. First, under this assumption, the Boolean model, $\mathcal{B}$, is used to check for blockages on the LOS path between $\mathbf{b}$ and $\mathbf{m}$ and is also used to find reflections, regardless of whether a path is blocked under $\mathcal{B}$. Then, to determine whether a reflection path is visible, the incident and reflected portions are separately checked for blockages under new, separate, i.i.d. Boolean models. This is formally outlined below.

Definition 6. *(Independent Blocking, Direct Path)* Let $\mathcal{B}$ be a Boolean model. We say that a *direct path* between points $\mathbf{p}$ and $\mathbf{q}$ is *visible* (or *not blocked*) if $\mathcal{B} \cap \mathcal{L}_{[\mathbf{p},\mathbf{q}]} = \emptyset$.[7]

Definition 7. *(Independent Blocking, Reflection Path)* Let $\mathcal{B}_1$ and $\mathcal{B}_2$ be i.i.d. Boolean models. We say that a *reflection path* between $\mathbf{b}$ and $\mathbf{m}$ with reflection point at $\mathbf{r}$, *i.e.*, $\mathcal{L}_{[\mathbf{b},\mathbf{r}]} \cup \mathcal{L}_{[\mathbf{r},\mathbf{m}]}$, is *visible* if $(\mathcal{B}_1 \cap \mathcal{L}_{[\mathbf{b},\mathbf{r}]}) \cup (\mathcal{B}_2 \cap \mathcal{L}_{[\mathbf{r},\mathbf{m}]}) = \emptyset$.

Lemma 2. *(Visible Direct Path) Consider Definition 6, then*

$$P[\mathcal{B} \cap \mathcal{L}_{[\mathbf{p},\mathbf{q}]} = \emptyset] = e^{-\lambda \mathbb{E}_{W,\Theta}\left[\mu_2\left(\mathcal{L}_{[\mathbf{p},\mathbf{q}]} \oplus R_{W,\Theta,\mathbf{0}}\right)\right]},$$

where $\mu_2(\mathcal{L}_{[\mathbf{p},\mathbf{q}]} \oplus R_{w,\theta,\mathbf{0}}) =$

$$\begin{cases} \sqrt{2}\, w\|\mathbf{p}-\mathbf{q}\| \sin(\pi/4 + \theta - \eta) + w^2 & 0 \leq \theta - \eta \leq \pi/2 \\ \sqrt{2}\, w\|\mathbf{p}-\mathbf{q}\| \left|\sin(-\pi/4 + \theta - \eta)\right| + w^2 & \text{otherwise,} \end{cases}$$

and $\eta = \tan^{-1}\left[([\mathbf{q}]_2 - [\mathbf{p}]_2)/([\mathbf{q}]_1 - [\mathbf{p}]_1)\right]$.

Proof. First, $\mu_2(\mathcal{L}_{[\mathbf{p},\mathbf{q}]} \oplus R_{w,\theta,\mathbf{0}})$ can be derived via simple geometric arguments [3], and by considering cases arising from the angle, η, of the slope of $\mathcal{L}_{[\mathbf{p},\mathbf{q}]}$ relative to the orientation of $R_{w,\theta,\mathbf{0}}$. Next, perform an independent thinning of Φ by retaining only the center points corresponding to reflectors of width, w, and orientation, θ, *i.e.*, $\Phi_{w,\theta} \subset \Phi$ with thinned density $\lambda f_{W,\Theta}(w,\theta)$. Then, $P[\mathcal{B} \cap \mathcal{L}_{[\mathbf{p},\mathbf{q}]} = \emptyset]$

$$\overset{(a)}{=} \prod_{i=1}^{n_w}\prod_{j=1}^{n_\theta} P[\Phi_{w_i,\theta_j}(\mathcal{L}_{[\mathbf{p},\mathbf{q}]} \oplus R_{w_i,\theta_j,\mathbf{0}}) = 0]$$
$$\overset{(b)}{=} e^{-\lambda \sum_{i=1}^{n_w}\sum_{j=1}^{n_\theta} f_{W,\Theta}(w_i,\theta_j)\,\mu_2\left(\mathcal{L}_{[\mathbf{p},\mathbf{q}]} \oplus R_{w,\theta,\mathbf{0}}\right)},$$

where (a) follows from independent thinning and (b) by the void probability of a PPP. The lemma follows. ■

Corollary 1. *(Visible LOS Path)*

$$P[\mathcal{B} \cap \mathcal{L}_{[\mathbf{b},\mathbf{m}]} = \emptyset] = e^{-\lambda\left(\sqrt{2}d\, \mathbb{E}_{W,\Theta}\left[W \sin(\pi/4+\Theta)\right] + \mathbb{E}_W\left[W^2\right]\right)}.$$

[7]One can interpret $\mathcal{B}$ as *random* or as a *realization*. We use the same notation for both cases. Its usage will be clear from context. This is analogous to using 'X' to refer to both the random variable, X, and its realization $X = x$.

Corollary 2. *(Visible Reflection Path) Consider Definition 7. Given Assumption 3,* $P[\mathcal{L}_{[\mathbf{b},\mathbf{r}]} \cup \mathcal{L}_{[\mathbf{r},\mathbf{m}]}$ is visible$] =$

$$e^{-\lambda \mathbb{E}_{W,\Theta}\left[\mu_2\left(\mathcal{L}_{[\mathbf{b},\mathbf{r}]} \oplus R_{W,\Theta,\mathbf{0}}\right) + \mu_2\left(\mathcal{L}_{[\mathbf{r},\mathbf{m}]} \oplus R_{W,\Theta,\mathbf{0}}\right)\right]}.$$

Proof. By Assumption 3 we have: $P[\mathcal{L}_{[\mathbf{b},\mathbf{r}]} \cup \mathcal{L}_{[\mathbf{r},\mathbf{m}]}$ is visible$] = P[\mathcal{L}_{[\mathbf{b},\mathbf{r}]}$ is visible$]P[\mathcal{L}_{[\mathbf{r},\mathbf{m}]}$ is visible$]$. Applying Lemma 2 yields the corollary. ■

Theorem 1. *(Number of Hearable, Visible Reflectors) Consider* $\mathbf{b}$ *and* $\mathbf{m}$ *under Boolean model,* $\mathcal{B}$*. Let* $V_{d_{max}}$ *denote the number of reflectors producing hearable, visible reflections between* $\mathbf{b}$ *and* $\mathbf{m}$*. Given independent blocking under Assumption 3,* $V_{d_{max}} \sim$ *Poisson*$(\mathbb{E}[V_{d_{max}}])$*, where* $\mathbb{E}[V_{d_{max}}] =$

$$2\lambda \sum_{j=1}^{n_\theta}\left[\int_{[\mathbf{m}_{\theta_j}]_1}^{[\mathbf{h}_{\mathrm{I}_{\theta_j}}]_1} p_{\mathrm{I}}(\mathbf{r}_{\mathrm{I}}(x_{\theta_j}))\mathrm{d}x_{\theta_j} + \int_{[\mathbf{b}_{\theta_j}]_2}^{[\mathbf{h}_{\mathrm{II}_{\theta_j}}]_2} p_{\mathrm{II}}(\mathbf{r}_{\mathrm{II}}(y_{\theta_j}))\mathrm{d}y_{\theta_j}\right]\sum_{i=1}^{n_w} w_i f_{W,\Theta}(w_i,\theta_j),$$

$[\mathbf{m}_{\theta_j}]_1 = [\mathbf{R}(\theta_j)\mathbf{m}]_1$, $[\mathbf{h}_{\mathrm{I}_{\theta_j}}]_1 = [\mathbf{R}(\theta_j)\mathbf{h}_{\mathrm{I}}]_1$, $[\mathbf{b}_{\theta_j}]_2 = [\mathbf{R}(\theta_j)\mathbf{b}]_2$, $[\mathbf{h}_{\mathrm{II}_{\theta_j}}]_2 = [\mathbf{R}(\theta_j)\mathbf{h}_{\mathrm{II}}]_2$,

$$p_{\mathrm{I}}(\mathbf{r}_{\mathrm{I}}(x_{\theta_j})) = P[\mathcal{L}_{[\mathbf{b},\mathbf{r}_{\mathrm{I}}(x_{\theta_j})]} \cup \mathcal{L}_{[\mathbf{r}_{\mathrm{I}}(x_{\theta_j}),\mathbf{m}]} \text{ is visible}], \quad (1)$$
$$p_{\mathrm{II}}(\mathbf{r}_{\mathrm{II}}(y_{\theta_j})) = P[\mathcal{L}_{[\mathbf{b},\mathbf{r}_{\mathrm{II}}(y_{\theta_j})]} \cup \mathcal{L}_{[\mathbf{r}_{\mathrm{II}}(y_{\theta_j}),\mathbf{m}]} \text{ is visible}],$$
$$\mathbf{r}_{\mathrm{I}}(x_{\theta_j}) = \frac{1}{4x_{\theta_j}}\begin{bmatrix}(4x_{\theta_j}^2 + d^2\sin^2\theta_j)\cos\theta_j \\ (4x_{\theta_j}^2 - d^2\cos^2\theta_j)\sin\theta_j\end{bmatrix}, \text{ and} \quad (2)$$
$$\mathbf{r}_{\mathrm{II}}(y_{\theta_j}) = \frac{1}{4y_{\theta_j}}\begin{bmatrix}-(4y_{\theta_j}^2 + d^2\cos^2\theta_j)\sin\theta_j \\ (4y_{\theta_j}^2 - d^2\sin^2\theta_j)\cos\theta_j\end{bmatrix}.$$

Proof. For $\mathcal{B}$, consider the thinned PPP of reflector centers, $\Phi_{w,\theta} \subset \Phi$, described in the proof of Lemma 2. We further thin this PPP by retaining only the center points corresponding to reflectors that produce visible reflections. By the independent blocking assumption, this is *independent* thinning; however, it is *location dependent*, *i.e.*, whether a point is retained depends on whether its corresponding reflector's edge e_i intersects the reflection hyperbola in Q_i and on whether the reflection is visible. We denote this thinned, *inhomogeneous* PPP by $\Phi_{v,w,\theta}$ (intensity measure $\Lambda_{v,w,\theta}$), where $\Phi_{v,w,\theta} \subset \Phi_{w,\theta}$. This yields $V_{d_{max}} = \sum_{i=1}^{n_w}\sum_{j=1}^{n_\theta} \Phi_{v,w_i,\theta_j}(\Omega(w_i,\theta_j,d_{max}))$. Since, the $\Phi_{v,w_i,\theta_j}(\Omega(w_i,\theta_j,d_{max}))$ are independent, Poisson random variables, then so is $V_{d_{max}}$. Taking the expectation:

$$\mathbb{E}[V_{d_{max}}] = \sum_{i=1}^{n_w}\sum_{j=1}^{n_\theta} \Lambda_{v,w_i,\theta_j}(\Omega(w_i,\theta_j,d_{max}))$$
$$= \sum_{i=1}^{n_w}\sum_{j=1}^{n_\theta}\sum_{q=\mathrm{I}}^{\mathrm{IV}} \Lambda_{v,w_i,\theta_j}(\Omega_q(w_i,\theta_j,d_{max}) + \mathbf{k}_q),$$

where the second equality follows from the Def. 5 remark.

We begin with $\Lambda_{v,w_i,\theta_j}(\Omega_{\mathrm{I}}(w_i,\theta_j,d_{max}) + \mathbf{k}_{\mathrm{I}})$. Since Φ_{v,w_i,θ_j} is obtained from Φ_{w_i,θ_j} via location dependent thinning, then if $p(\mathbf{y})$ is our retention probability (a continuous function over $\Omega_{\mathrm{I}} + \mathbf{k}_{\mathrm{I}}$), we have $\Lambda_{v,w_i,\theta_j}(\Omega_{\mathrm{I}}(w_i,\theta_j,d_{max}) + \mathbf{k}_{\mathrm{I}})$

$$\overset{(a)}{=} \int_{\Omega_{\mathrm{I}}(w_i,\theta_j,d_{max})+\mathbf{k}_{\mathrm{I}}} p(\mathbf{y})\,\mathrm{d}\Lambda_{w_i,\theta_j} \overset{(b)}{=} \int_{\Omega_{\mathrm{I}}(w_i,\theta_j,d_{max})} p(\mathbf{x}+\mathbf{k}_{\mathrm{I}})\,\mathrm{d}\Lambda_{w_i,\theta_j}$$
$$\overset{(c)}{=} \int_{\Omega_{\mathrm{I}}(w_i,\theta_j,d_{max})} p_{\mathrm{I}}(\mathbf{x})\,\mathrm{d}\Lambda_{w_i,\theta_j} \overset{(d)}{=} \lambda f_{W,\Theta}(w_i,\theta_j)\int_{\Omega_{\mathrm{I}}(w_i,\theta_j,d_{max})} p_{\mathrm{I}}(\mathbf{x})\,\mathrm{d}\mathbf{x}, \quad (3)$$

where (a) follows by definition, (b) by setting $\mathbf{x} = \mathbf{y} - \mathbf{k}_{\mathrm{I}}$, (c) by setting $p_{\mathrm{I}}(\mathbf{x}) = p(\mathbf{x} + \mathbf{k}_{\mathrm{I}})$, and (d) from $\Lambda_{w_i,\theta_j}(B) = \lambda f_{W,\Theta}(w_i,\theta_j)\mu_2(B)$, for all Borel sets, B, and from the continuity of p. Note, the steps (b) and (c) imply: if $\mathbf{x} \in \Omega_{\text{I}}(w_i, \theta_j, d_{max})$, then $\mathbf{y} \in \Omega_{\text{I}}(w_i, \theta_j, d_{max}) + \mathbf{k}_{\text{I}}$ and $p(\mathbf{y}) = p_{\text{I}}(\mathbf{x})$; *i.e.*, both points have the same retention probability. If we consider $\Phi_{w_i,\theta_j} - \mathbf{k}_{\text{I}}$, the PPP of center points *of the reflectors' edges* e_{I}, then p_{I} is the retention probability of these edge centers. Thus, $p(\mathbf{y}) = p_{\text{I}}(\mathbf{x})$ implies the PPP of edge-e_{I} centers over Ω_{I} is thinned equivalently to the PPP of reflector centers over $\Omega_{\text{I}} + \mathbf{k}_{\text{I}}$.

To find p_{I}, from $\Phi_{w_i,\theta_j} - \mathbf{k}_{\text{I}}$ over the region $\Omega_{\text{I}}(w_i, \theta_j, d_{max})$, we turn to Fig. 2. Considering a coordinate system rotated by θ_j, then all of the points in the slice x_{θ_j} have the same retention probability, since the center of edge e_{I} can lie anywhere in this slice to produce a reflection at $\mathbf{r}_{\text{I}}(x_{\theta_j})$. Thus, in this rotated system, (3) reduces to

$$= \lambda w_i f_{W,\Theta}(w_i, \theta_j) \int_{[\mathbf{m}_{\theta_j}]_1}^{[\mathbf{h}_{\text{I}_{\theta_j}}]_1} p_{\text{I}}(\mathbf{r}_{\text{I}}(x_{\theta_j}))\, \mathrm{d}x_{\theta_j},$$

where $[\mathbf{m}_{\theta_j}]_1 = [\mathbf{R}(\theta_j)\mathbf{m}]_1$, $[\mathbf{h}_{\text{I}_{\theta_j}}]_1 = [\mathbf{R}(\theta_j)\mathbf{h}_{\text{I}}]_1$, and $p_{\text{I}}(\mathbf{r}_{\text{I}}(x_{\theta_j}))$ is the probability that the center point of edge e_{I}, $\mathbf{x}_{\theta_j}$ with $[\mathbf{x}_{\theta_j}]_1 = x_{\theta_j}$, is retained, *i.e.*, it is the probability that the corresponding reflector of this 'edge-e_{I} center point' facilitates a visible reflection at point $\mathbf{r}_{\text{I}}(x_{\theta_j})$. Hence, by Corollary 2, we have (1). The reflection point $\mathbf{r}_{\text{I}}$ as a function of x_{θ_j} is derived by finding $\mathcal{H}_{\theta_j}$ in the rotated coordinate system: $y_{\theta_j} = -d^2 \sin(2\theta_j)/(8x_{\theta_j})$, finding the reflection point in this coordinate system: $\mathbf{r}_{\text{I}_{\theta_j}}(x_{\theta_j}) = [x_{\theta_j}, -d^2 \sin(2\theta_j)/(8x_{\theta_j})]^T$, and then rotating it back to the original system: $\mathbf{r}_{\text{I}}(x_{\theta_j}) = (\mathbf{R}(\theta_j))^{-1}\mathbf{r}_{\text{I}_{\theta_j}}(x_{\theta_j})$, yielding (2).

Note, $\Lambda_{v,w_i,\theta_j}(\Omega_{\text{II}}(w_i, \theta_j, d_{max}) + \mathbf{k}_{\text{II}})$ is obtained analogously and symmetry implies $\Lambda_{v,w_i,\theta_j}(\Omega_{\text{I}}+\mathbf{k}_{\text{I}}) = \Lambda_{v,w_i,\theta_j}(\Omega_{\text{III}}+\mathbf{k}_{\text{III}})$ and $\Lambda_{v,w_i,\theta_j}(\Omega_{\text{II}}+\mathbf{k}_{\text{II}}) = \Lambda_{v,w_i,\theta_j}(\Omega_{\text{IV}}+\mathbf{k}_{\text{IV}})$. ∎

Corollary 3. *(The Localization Probability) Given single-anchor localization with the anchor and mobile separated by d meters, a Boolean model of reflectors, and a hearability distance of d_{max} meters, then* P[The mobile can be localized] =

$$\underbrace{P[\mathcal{B} \cap \mathcal{L}_{[\mathbf{b},\mathbf{m}]} = \emptyset]}_{\text{P[LOS is Visible]}} + \underbrace{\left(1 - P[\mathcal{B} \cap \mathcal{L}_{[\mathbf{b},\mathbf{m}]} = \emptyset]\right) P[V_{d_{max}} \geq 2]}_{\text{P[LOS Blocked, but Sufficient NLOS Paths]}}.$$

Proof. This follows by Assumptions 3 and 4. ∎

V. Numerical Results

The three simulations in Fig. 3 were conducted in the same manner as discussed in the first paragraph of Sec. IV. The only difference was in how reflected paths were checked for blockages. For blocking under Assumption 3, the incident and reflected paths for each reflection were checked for blockages under new, i.i.d. Boolean model realizations; for independent blocking from [4], [5], [6], each reflected path uses a new, i.i.d. Boolean model realization to check for blockages along the entirety of the path; and lastly, for correlated blocking (true blocking), the original Boolean model, $\mathcal{B}$, is used to check for blockages on all reflected paths.

First, note that the simulation with Assumption 3 blocking matches Corollary 3, supporting the analytical derivation. Next, we see that Assumption 3 blocking better approximates the true, correlated blocking scenario than does the blocking assumption in the references. This is due to the 'overestimation' of the region where a reflector may fall to produce a blockage (see Corollary 2), leading to a higher blocking probability more in line with true, correlated blocking. Further, NLOS localization appears to be a small contributer to the overall single-anchor localization probability. However, [1] does note that even when a location estimate is obtained, each additional NLOS path still contributes to a reduction in position error. Thus, Theorem 1 can also be used to roughly quantify how much position error reduction is available.

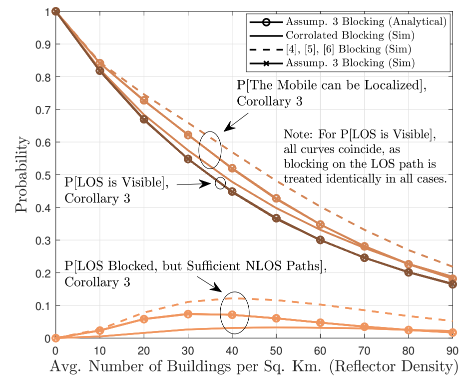

Fig. 3. Analytical Vs. Simulation. Parameters: $d = 200m$, $d_{max} = 1km$, and the reflectors (buildings) were chosen from the joint uniform distribution, $f_{W,\Theta}(w, \theta) = 1/(5 \cdot 8)$, where $\text{supp}(f_{W,\Theta}) = \{ [w, \theta]^T \in \mathbb{R}^2 \,|\, w \in \{20m, 40m, \ldots, 100m\}, \theta \in \{10°, 20°, \ldots, 80°\} \}$. This implies $\mathbb{E}[W] = 60m$ and that roughly, for example, an avg. of 32% of the land is covered by buildings at the density of 90 buildings/sq. km. Simulated probabilities were generated over 10^5 Boolean model realizations on a $1.3km \times 1.3km$ grid.

VI. Conclusion

For a single anchor-mobile pair, this paper utilizes the Boolean model to analytically derive the probability that the mobile can obtain an unambiguous location estimate. This localization probability not only accounts for LOS localization, but also accounts for the possibility of localization via NLOS signals exclusively. Finally, this result reveals that in the absence of LOS, the probability of having sufficient NLOS signals to localize is relatively small.

References

[1] R. Mendrzik, H. Wymeersch, G. Bauch, and Z. Abu-Shaban, "Harnessing NLOS components for position and orientation estimation in 5G millimeter wave MIMO," in *IEEE Trans. on Wireless Commun.*, vol. 18, no. 1, pp. 93-107, Jan. 2019.

[2] J. G. Andrews, T. Bai, M. N. Kulkarni, A. Alkhateeb, A. K. Gupta, and R. W. Heath, "Modeling and analyzing millimeter wave cellular systems," in *IEEE Trans. on Commun.*, vol. 65, no. 1, pp. 403-430, Jan. 2017.

[3] T. Bai, R. Vaze, and R. W. Heath, "Analysis of blockage effects on urban cellular networks," in *IEEE Trans. on Wireless Commun.*, vol. 13, no. 9, pp. 5070-5083, Sept. 2014.

[4] N. A. Muhammad, P. Wang, Y. Li, and B. Vucetic, "Analytical model for outdoor millimeter wave channels using geometry-based stochastic approach," in *IEEE Trans. on Veh. Technol.*, vol. 66, no. 2, pp. 912-926, Feb. 2017.

[5] R. T. Rakesh, G. Das, and D. Sen, "An analytical model for millimeter wave outdoor directional non-line-of-sight channels," in *Proc. of the IEEE International Conf. on Commun. (ICC)*, Paris, France, May 2017, pp. 1-6.

[6] M. Dong and T. Kim, "Interference analysis for millimeter-wave networks with geometry-dependent first-order reflections," in *IEEE Trans. on Veh. Technol.*, vol. 67, no. 12, pp. 12404-12409, Dec. 2018.

[7] A. Narayanan, S. T. Veetil, and R. K. Ganti, "Coverage analysis in millimeter wave cellular networks with reflections," in *Proc. of the IEEE Global Commun. Conf.*, Singapore, Dec. 2017, pp. 1-6.

[8] C. E. O'Lone, H. S. Dhillon, and R. M. Buehrer, "A mathematical justification for exponentially distributed NLOS bias," in *Proc. of the IEEE Global Commun. Conf.*, 2019. Available online: arxiv.org/abs/1905.00603.

[9] J. Schloemann, H. S. Dhillon, and R. M. Buehrer, "Towards a tractable analysis of localization fundamentals in cellular networks," in *IEEE Trans. on Wireless Commun.*, vol. 15, no. 3, pp. 1768-1782, Mar. 2016.